Supplementary Materials

of

Ship emission of nitrous acid (HONO) and its impacts on the marine atmospheric oxidation chemistry

Lei Sun[a,b#], Tianshu Chen[a#], Ying Jiang[a], Yang Zhou[c], Lifang Sheng[c], Jintai Lin[d], Juan Li[a], Can Dong[a], Chen, Wang[b], Xinfeng Wang[a], Qingzhu Zhang[a], Wenxing Wang[a], Likun Xue[a*]

[a] Environment Research Institute, Shandong University, Qingdao, Shandong, China

[b] School of Environmental Science & Engineering, Qilu University of Technology (Shandong Academy of Sciences), Ji'nan, Shandong, China

[c] Key Laboratory of Physical Oceanography, College of Oceanic and Atmospheric Sciences, Ocean University of China, Qingdao, Shandong, China

[d] Department of Atmospheric and Oceanic Sciences, School of Physics, Peking University, Beijing, China

#These authors contributed equally to this work.

*Corresponding author: Likun Xue (xuelikun@sdu.edu.cn)

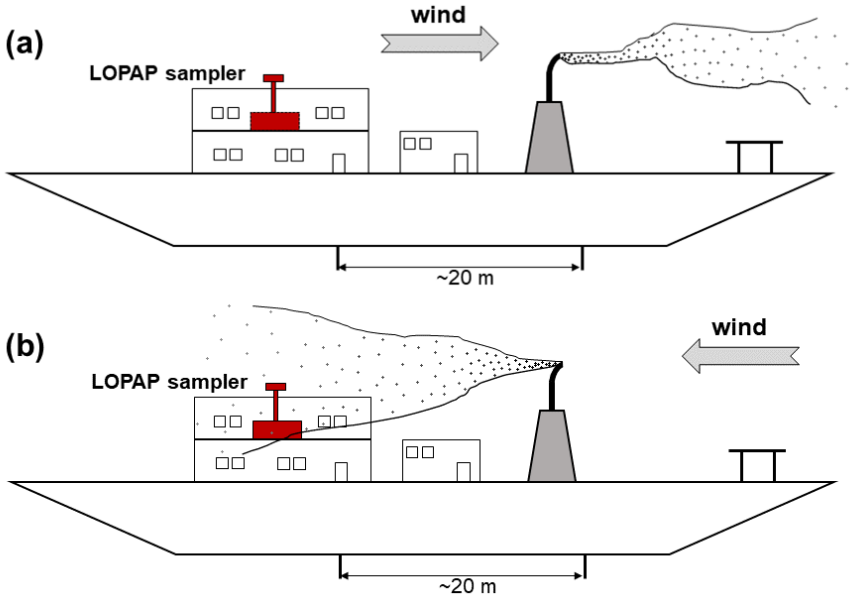

Figure S1. Schematic diagram of the sampling inlet unaffected (a) or affected (b) by ship plumes when the vessel stopped.

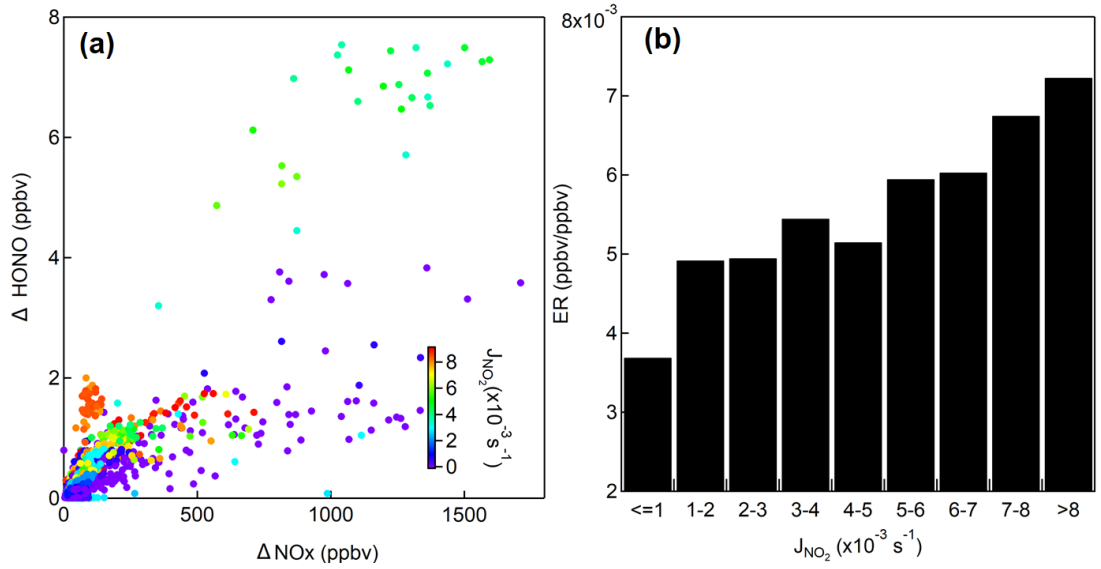

Figure S2. (a) Scatter plot of HONO versus NO_x for the ship plume data. The color bar indicates the intensity of J_{NO2} that was concurrently measured during the experiment period. (b) Category plot of ER ($\Delta HONO/\Delta NO_x$) versus J_{NO2}.

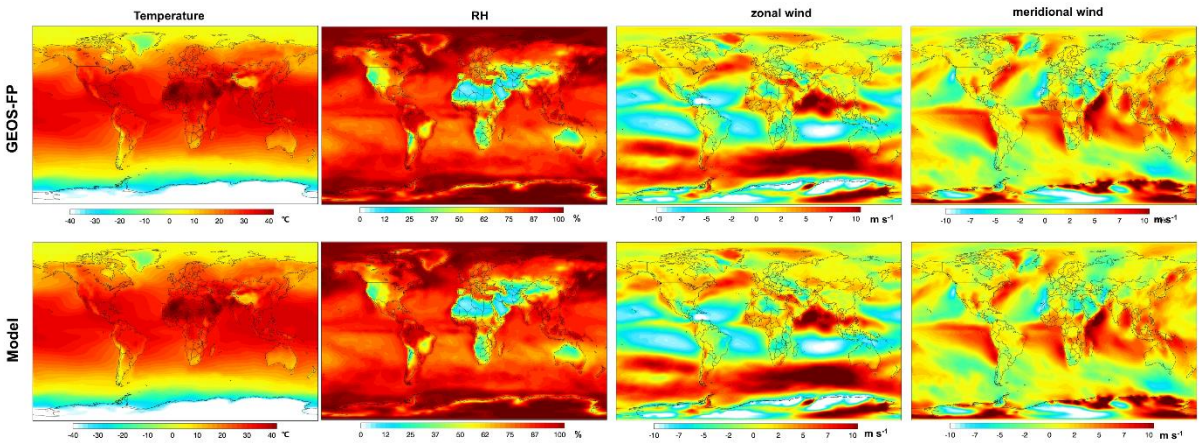

Figure S3. Monthly average of 2-m temperature, relative humidity, the zonal wind (positive for eastward) and the meridional wind (positive for northward) in July 2014 from GEOS-FP meteorological field and GEOS-Chem.

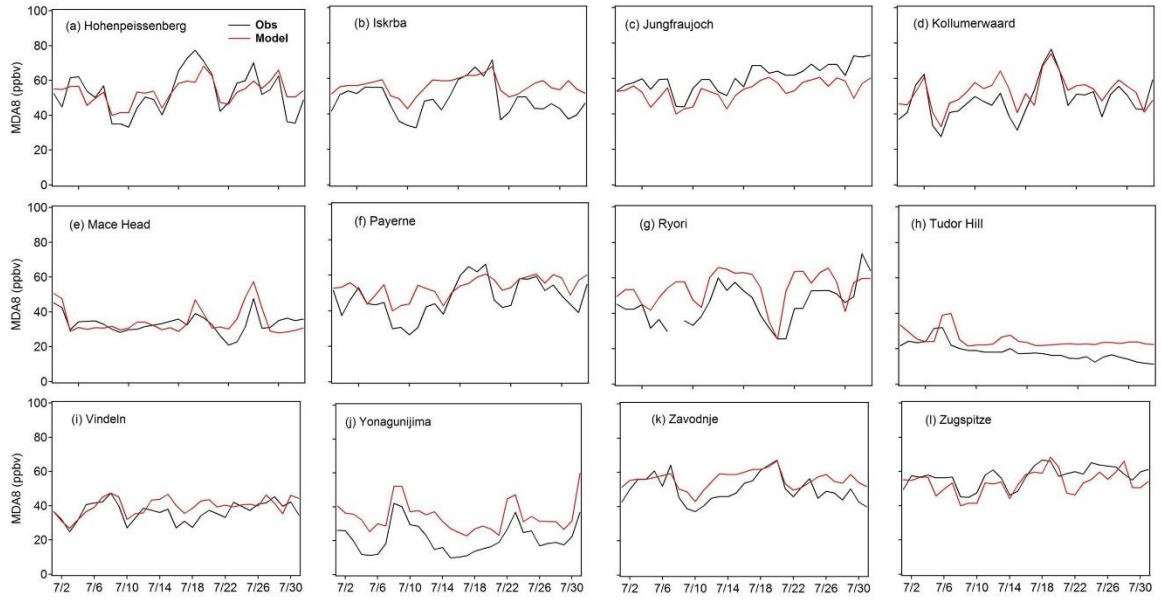

Figure S4. Time series of simulated and observed MDA8 O_3 at remote and rural sites in July 2014. The model reproduces the variations of observed data.

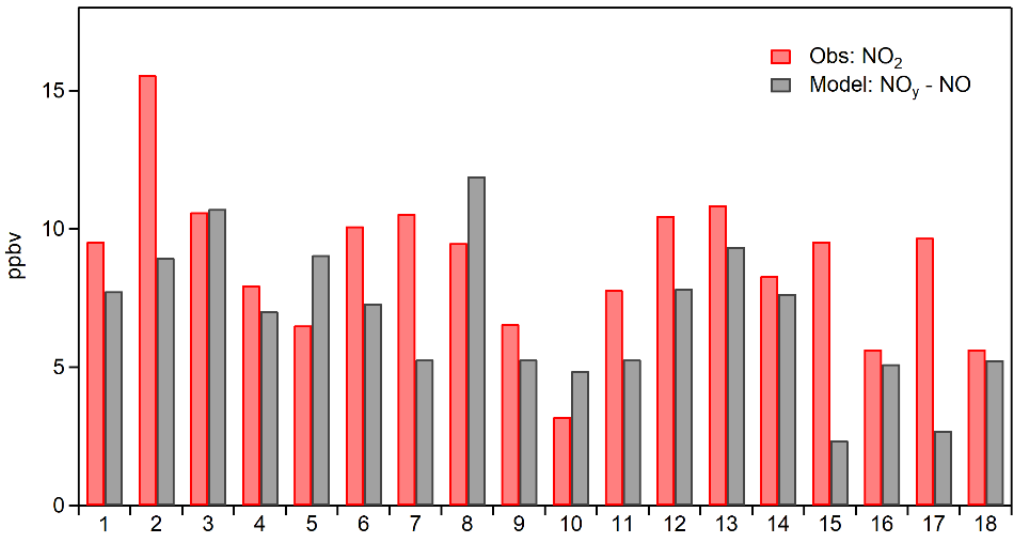

Figure S5. Monthly average of observed NO_2 and simulated (NO_y-NO) at 19 sites in China. The overestimation was mainly due to the catalytic conversion of other oxidized nitrogen species to NO (Xu et al., 2013). The underestimation was mainly due to the low model resolution that cannot capture variations of local emissions (Sun et al., 2019). The 19 sites covered different regions of China mainland: 1. Beijing, 2. Tianjin, 2. Ji'nan， 4. Qingdao and 5. Xuzhou for North China; 6. Shenyang and 7. Dalian for Northeast China; 8. Hangzhou, 9. Ningbo and 10. Fuzhou for Southeast China; 11. Nanchang, 12. Wuhan and13. Hefei for Central China; 14. Guangzhou and 15. Nanning for South China; 16. Xi'an and 17. Lanzhou for Northwest China; and 18. Chengdu for Southwest China.

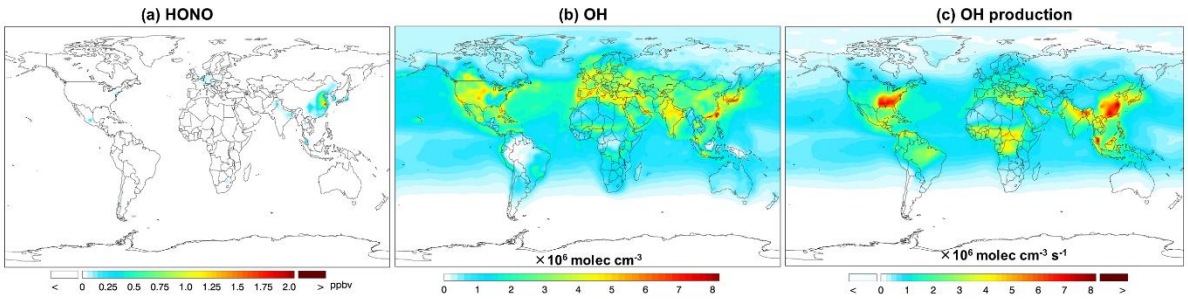

Figure S6. Model-simulated monthly-mean spatial distributions of (a) HONO, (b) OH, and (c) total primary OH production rate in July 2014 from the Base Scenario.

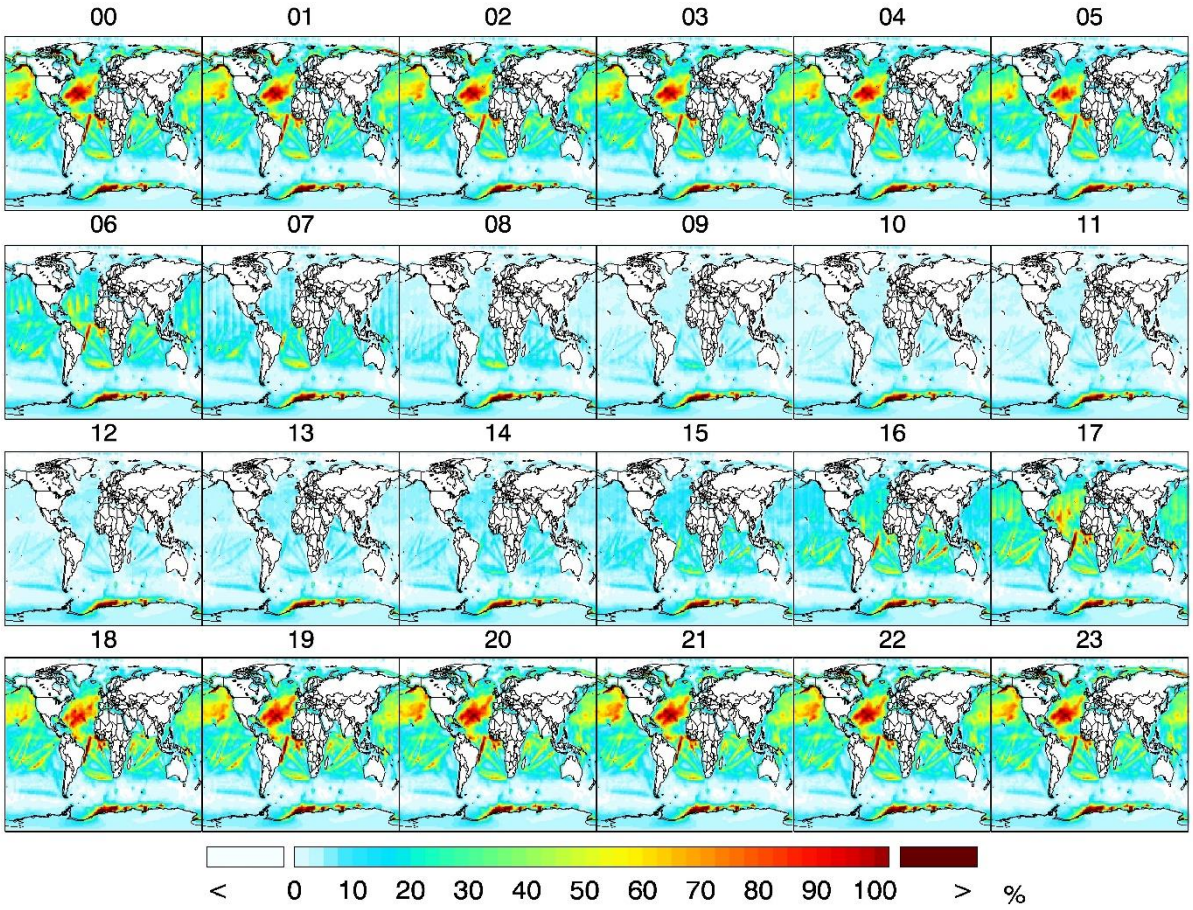

Figure S7. Model-simulated monthly-mean percent difference between Base and Test simulations of hourly HONO spatial distributions. The difference represents the ratio of absolute difference versus Base simulation ((Test-Base)/Base*100%).

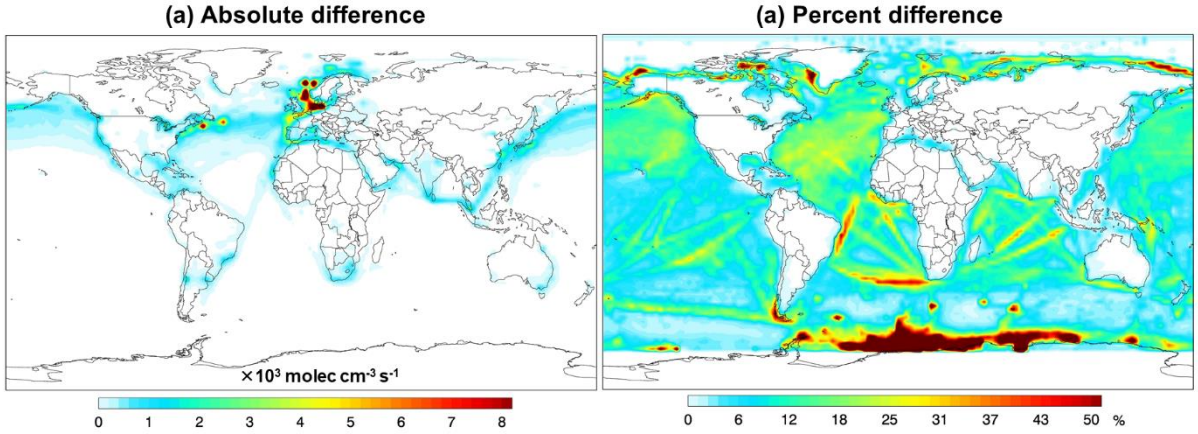

Figure S8. Model-simulated absolute and percent differences between Test simulation and Base simulation of monthly-mean spatial distributions of OH production rate from HONO photolysis.

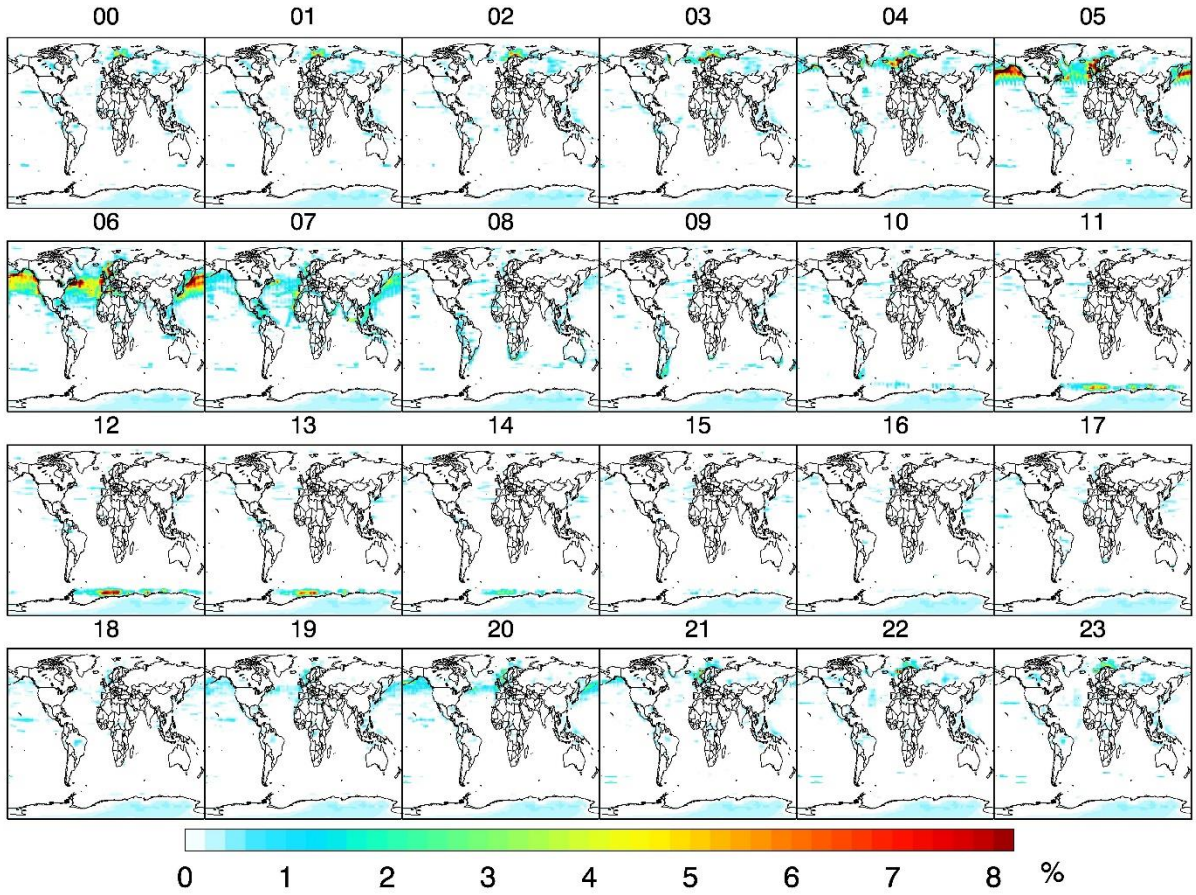

Figure S9. Model-simulated monthly-mean percent difference between Base and Test simulations of hourly total primary OH sources.

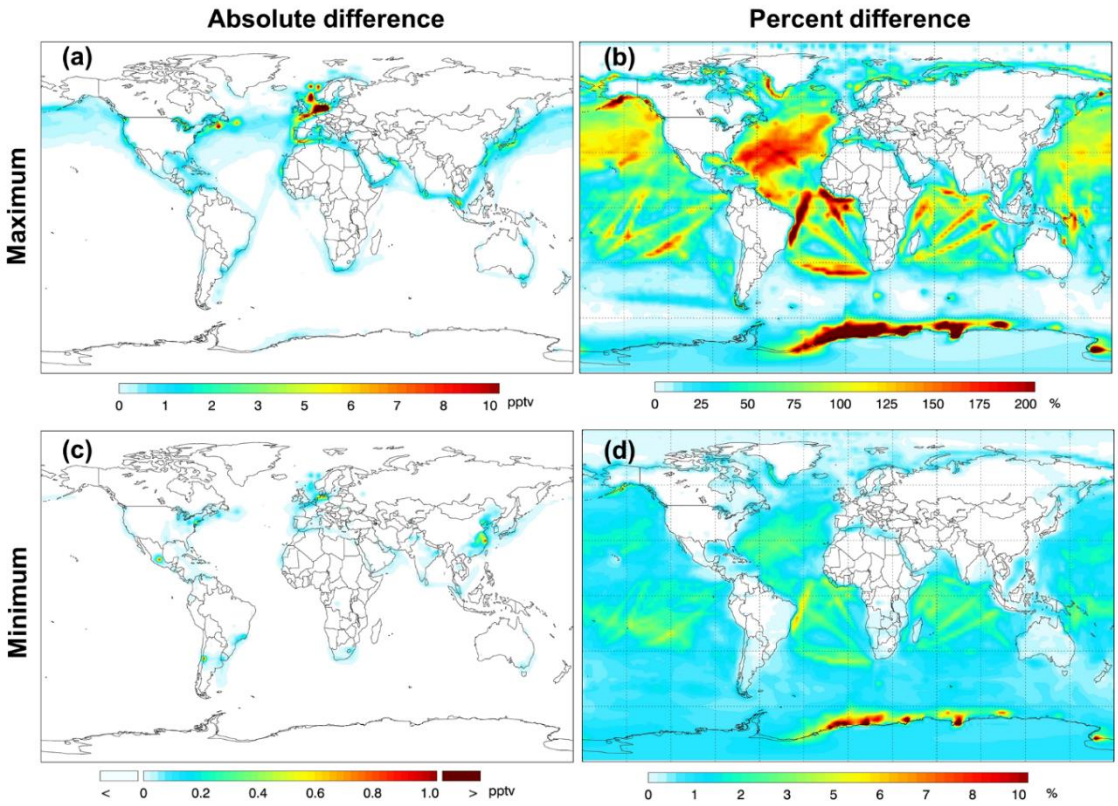

Figure S10. Model simulated monthly-mean absolute difference and percent difference between Base and Test simulations of HONO concentrations based on the ER=1.7% ((a) and (b)) and 0.03% ((c) and (d)).

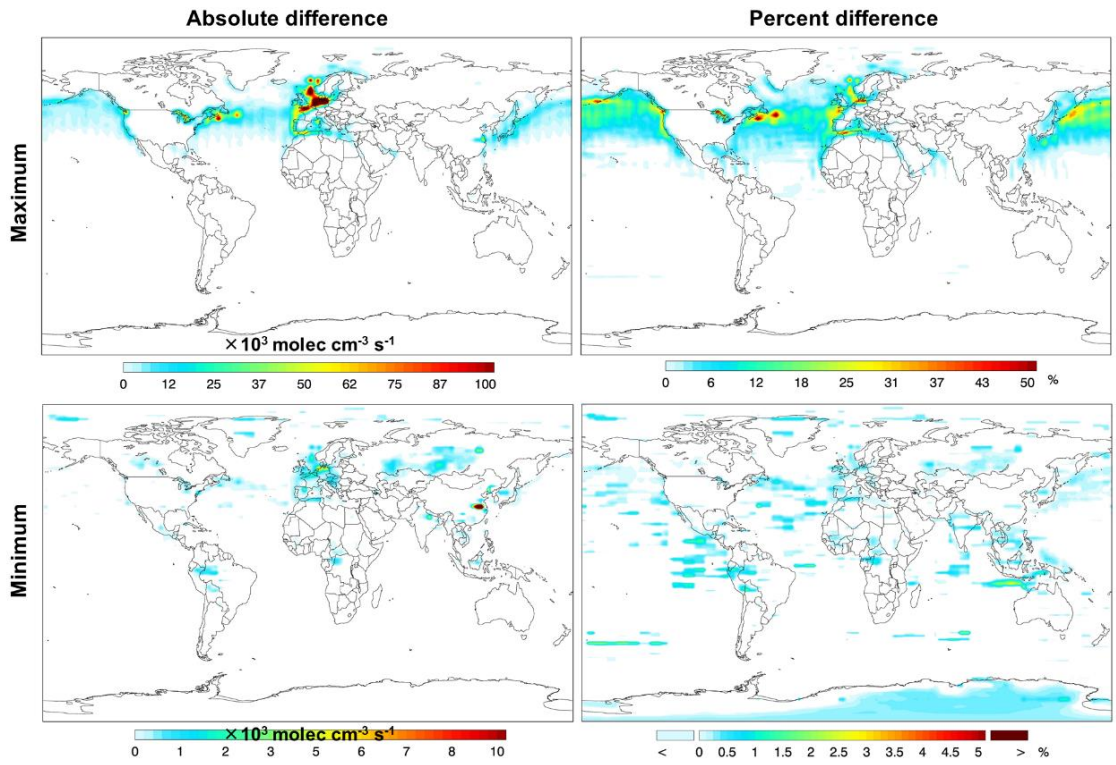

Figure S11. Model simulated monthly-mean absolute difference and percent difference of primary OH sources between Base and Test simulations based on the ER=1.7% ((a) and (b)) and 0.03% ((c) and (d)).

Table S1. Summary of the traffic-induced, exhaust-induced, and ship plume HONO/NO_x ratios from literatures.

Method	Object	Instrument	Type	HONO/NO_x	Reference
Chassis dynamo meter	light duty motor vehicle (LDMV)	DOAS	Eight different LDMV with spark ignition engines	0.1–0.8%	Pitts et al.,1984
	Gosoline Vehicle	CEAS	Six different light vehicles	0.11–0.68%	Nakashima and Kajii,2017
	Gasoline/diesel vehicle	ADAMD	Two different vehicles	Gasoline:0–0.95% Diesel: 0.16–1.0%	Trinh et al., 2017
	Gasoline vehicle	LOPAP	Different engines	0.03–0.42%	Liu et al., 2017
Tunnel experiment	Caldecott Tunnel, United States	Na_2CO_3-coated glass annular denuder	>99% gasoline-fueled, <2% heavy-duty vehicle	(0.29 ±0.05)%	Kirchstetter et al., 1996
	Wuppertal Kiesbergtunnel, Germany	DOAS	75% gasoline and 12% diesel cars	(0.8 ±0.1)%	Kurtenbach et al., 2011
	Shing Mun Tunnel, Hong Kong, China	LOPAP	47% gasoline, 38% diesel and 15% LPG vehicle	(1.24 ±0.35)%	Liang et al., 2017
Measurement site near road	Mong Kok, Hong Kong,China	LOPAP	42% gasoline, 26% diesel and 23% LPG vehicle	(1 ±0.5)%	Yun et al., 2017
	Tung Chung, Hong Kong, China	LOPAP	33% diesel and 67% gasoline vehicles	1.20%	Xu et al., 2015
	Highway junction, Houston, United States	LOPAP	89-95% gasoline and 5%-11% diesel vehicle	1.70%	Rappengluck et al.,2013
	Urban site in Ji'nan	LOPAP	Near urban street	(0.53 ±0.20)%	Li et al., 2018
Ship plume	Exhaust of Ship, East China Sea	LOPAP	All ship plume	(0.46 ±0.31)%	This work
		LOPAP	Typical ship plume	(0.51 ±0.18)%	This work

Table S2: Monthly ship emissions of NO_x and HONO based on CEDS inventory and the ER of this study and references in Table S1 (Units: Gg $month^{-1}$).

Emissions	Jan.	Feb.	Mar.	Apr.	May	Jun.	Jul.	Aug.	Sept.	Oct.	Nov.	Dec.
NO_x	965	830	1012	972	1022	952	1050	1064	1014	1088	1059	1070
This study	5.10± 1.77	4.38± 1.53	5.34± 1.86	5.13± 1.79	5.39± 1.88	5.03± 1.75	5.54± 1.93	5.62± 1.96	5.35± 1.86	5.74± 2.00	5.59± 1.95	5.65± 1.97
ER= 1.7%	16.41	14.11	17.2	16.5	17.37	16.2	17.9	18.1	17.2	18.5	18	18.2
ER = 0.03%	0.289	0.249	0.304	0.29	0.307	0.29	0.32	0.32	0.3	0.326	0.32	0.32

Table S3. Comparison of simulated and observed MDA8 O_3 at 12 remote or rural sites.

Site	Location	Characteristics	Obs (ppbv) Mean ±SD	Model (ppbv) Mean ±SD	NMB (%)
Hohenpeissenberg	11.01 °N, 47.8 °E, 985 m	Remote	52.9±12.0	53.5±6.8	1.1
Iskrba	14.86 °N, 45.56 °E, 540 m	Rural	48.1±9.5	55.7±5.0	15.8
Jungfraujoch	7.985 °N, 46.547 °E, 3580 m	Remote	60.6±7.4	53.2±5.8	-12.2
Kollumerwaard	6.28 °N, 53.33 °E, 0 m	Remote	48.2±10.9	52.6±8.6	9.2
Mace Head	9.899 °S, 53.326 °E, 8 m	Remote	33.4±5.5	34.6±7.7	3.7
Payerne	6.94 °N, 46.81 °E, 489 m	Rural	47.2±10.5	53.2±5.8	12.7
Ryori	141.82 °N, 39.03 °E, 260 m	Remote	45.0±11.3	54.4±9.7	25
Tudor Hill	64.87 °S, 432.264 °E, 30 m	Suburban	18.3±5.0	25.0±4.6	36.2
Vindeln	19.767 °N, 64.25 °E, 225 m	Rural	36.6±5.6	39.7±5.1	8.4
Yonagunijima	123.02 °N, 24.47.8 °E, 30 m	Remote	21.3±8.9	34.3±9.0	60.8
Zavodnje	15 °N, 46.43 °E, 770 m	Remote	50.1±7.9	55.7±5.0	11.3
Zugspitze	10.98 °N, 47.42 °E, 2960 m	Remote	57.2±6.0	53.5±6.8	-6.6

Table S4. Comparison of simulated and observed HONO at 10 rural sites.

Site	Period	Obs (ppbv) Mean ±SD	References
Beijing，China (urban)	Jun. –Jul. 2016	1.38±0.90	Wang et al., 2017
Ji'nan, China (urban)	Jun. –Aug. 2016	1.12±0.93	Li et al., 2018a
Wangdu, China (rural)	Jun. –Jul. 2014	0.91±0.48	Liu et al., 2019
Back Garden, China (rural)	Jul. 2006	0.76	Li et al., 2012
Whiteface Mountain, USA (1483 m a.s.l.)	14 Jun. –20 Jul. 1999	0.046	Zhou et al., 2007
Hohenpeissenberg, Germany (980 m a.s.l.)	2 Jul. –12 Jul. 2002	0.039	Acker et al., 2006
	29 Jun. –14 Jul. 2004	0.063	Acker et al., 2006
Mt. Brocken, Germany (1142 m a.s.l.)	19 Jun. –4 Jul. 1999	0.056	Acker et al., 2001
Northern Michigan (1000-1900 m a.s.l.)	30 Jul. –6 Aug. 2007	0.009	Zhang et al., 2009
Northern Italy (300-1000 m a.g.l.)	12 Jul. 2012	~0.15	Li et al., 2014
Southeastern USA (>1500 m a.g.l.)	1 Jun. –15 Jul. 2013	0.006±0.003	Ye et al., 2018

References

Acker, K., Möller, D., Wieprecht, W., Auel, R., Kalass, D., Tscherwenka, W., 2001. Nitrous and Nitric Acid Measurements Inside and Outside of Clouds at Mt. Brocken. Water, Air, and Soil Pollution 130, 331–336.

Acker, K., Möller, D., Wieprecht, W., Meixner, F.X., Bohn, B., Gilge, S., Plass-Dülmer, C., Berresheim, H., 2006. Strong daytime production of OH from HNO_2 at a rural mountain site. Geophysical Research Letters 33.

Kirchstetter, T.W., Harley, R.A., Littlejohn, D., 1996. Measurement of Nitrous Acid in Motor Vehicle Exhaust. Environmental Science & Technology 30, 2843–2849.

Kurtenbach, R., Becker, K.H., Gomes, J.A.G., Kleffmann, J., Lörzer, J.C., Spittler, M., Wiesen, P., Ackermann, R., Geyer, A., Platt, U., 2001. Investigations of emissions and heterogeneous formation of HONO in a road traffic tunnel. Atmos. Enviro. 35, 3385–3394.

Li, D., Xue, L., Wen, L., Wang, X., Chen, T., Mellouki, A., Chen, J., Wang, W., 2018. Characteristics and sources of nitrous acid in an urban atmosphere of northern China: Results from 1-yr continuous observations. Atmos. Environ. 182, 296–306.

Li, X., Brauers, T., Häseler, R., Bohn, B., Fuchs, H., Hofzumahaus, A., Holland, F., Lou, S., Lu, K.D., Rohrer, F., Hu, M., Zeng, L.M., Zhang, Y.H., Garland, R.M., Su, H., Nowak, A., Wiedensohler, A., Takegawa, N., Shao, M., Wahner, A., 2012. Exploring the atmospheric chemistry of nitrous acid (HONO) at a rural site in Southern China. Atmos. Chem. Phys. 12, 1497–1513.

Li, X., Rohrer, F., Hofzumahaus, A., Brauers, T., Häseler, R., Bohn, B., Broch, S., Fuchs, H., Gomm, S., Holland, F., Jäger, J., Kaiser, J., Keutsch, F.N., Lohse, I., Lu, K., Tillmann, R., Wegener, R., Wolfe, G.M., Mentel, T.F., Kiendler-Scharr, A., Wahner, A., 2014. Missing Gas-Phase Source of HONO Inferred from Zeppelin Measurements in the Troposphere. Science 344, 292–296.

Liang, Y., Zha, Q., Wang, W., Cui, L., Lui, K.H., Ho, K.F., Wang, Z., Lee, S.-c., Wang, T., 2017. Revisiting nitrous acid (HONO) emission from on-road vehicles: A tunnel study with a mixed fleet. J. Air Waste Manage 67, 797–805.

Liu, Y., Lu, K., Ma, Y., Yang, X., Zhang, W., Wu, Y., Peng, J., Shuai, S., Hu, M., Zhang, Y., 2017. Direct emission of nitrous acid (HONO) from gasoline cars in China determined by vehicle chassis dynamometer experiments. Atmos. Environ. 169, 89–96.

Liu, Y., Lu, K., Li, X., Dong, H., Tan, Z., Wang, H., Zou, Q., Wu, Y., Zeng, L., Hu, M., Min, K.-E., Kecorius, S., Wiedensohler, A., Zhang, Y., 2019. A Comprehensive Model Test of the HONO Sources Constrained to Field Measurements at Rural North China Plain. Environmental Science & Technology 53, 3517–3525.

Nakashima, Y., Kajii, Y., 2017. Determination of nitrous acid emission factors from a gasoline vehicle using a chassis dynamometer combined with incoherent broadband cavity-enhanced absorption spectroscopy. Sci. Total Enviro. 575, 287–293.

Pitts, J.N., Biermann, H.W., Winer, A.M., Tuazon, E.C., 1984. Spectroscopic identification and measurement of gaseous nitrous acid in dilute auto exhaust. Atmospheric Environment (1967) 18, 847–854.

Rappenglück, B., Lubertino, G., Alvarez, S., Golovko, J., Czader, B., Ackermann, L., 2013. Radical precursors and related species from traffic as observed and modeled at an urban highway junction. J. Air Waste Manage 63, 1270–1286.

Sun, L., Xue, L., Wang, Y., Li, L., Lin, J., Ni, R., Yan, Y., Chen, L., Li, J., Zhang, Q., Wang, W., 2019. Impacts of meteorology and emissions on summertime surface ozone increases over central eastern China between 2003 and 2015. Atmos. Chem. Phys. 19, 1455-1469.

Trinh, H.T., Imanishi, K., Morikawa, T., Hagino, H., Takenaka, N., 2017. Gaseous nitrous acid (HONO) and nitrogen oxides (NO_x) emission from gasoline and diesel vehicles under real-world driving test cycles. J. Air Waste Manage 67, 412–420.

Wang, J., Zhang, X., Guo, J., Wang, Z., Zhang, M., 2017. Observation of nitrous acid (HONO) in Beijing, China: Seasonal variation, nocturnal formation and daytime budget. Science of The Total Environment 587-588, 350-359.

Xu, Z., Wang, T., Wu, J., Xue, L., Chan, J., Zha, Q., Zhou, S., Louie, P.K.K., Luk, C.W.Y., 2015. Nitrous acid (HONO) in a polluted subtropical atmosphere: Seasonal variability, direct vehicle emissions and heterogeneous production at ground surface. Atmos. Environ. 106, 100–109.

Ye, C., Zhou, X., Pu, D., Stutz, J., Festa, J., Spolaor, M., Tsai, C., Cantrell, C., Mauldin Iii, R.L., Weinheimer, A., Hornbrook, R.S., Apel, E.C., Guenther, A., Kaser, L., Yuan, B., Karl, T., Haggerty, J., Hall, S., Ullmann, K., Smith, J., Ortega, J., 2018. Tropospheric HONO distribution and chemistry in the southeastern US. Atmos. Chem. Phys. 18, 9107-9120.

Yun, H., Wang, Z., Zha, Q., Wang, W., Xue, L., Zhang, L., Li, Q., Cui, L., Lee, S., Poon, S.C., 2017. Nitrous acid in a street canyon environment: Sources and contributions to local oxidation capacity. Atmos. Environ. 167, 223–234.

Zhang, N., Zhou, X., Shepson, P.B., Gao, H., Alaghmand, M., Stirm, B., 2009. Aircraft measurement of HONO vertical profiles over a forested region. Geophysical Research Letters 36(15):172-173.

Zhou, X., Gu, H., Civerolo, K., Roychowdhury, U., Demerjian, K.L., 2007. Summertime observations of HONO, HCHO, and O_3 at the summit of Whiteface Mountain, New York. Journal of Geophysical Research Atmospheres 112, D08311, doi:10.1029/2006JD007256.